Supplementary Data

Guest induced transformations of assembled pyridyl *bis-urea* macrocycle.

Kinkini Roy,[a] Chun Wang,[a] Mark D. Smith,[a] Mahender B. Dewal,[a] Arief C.Wibowo,[a] Julius C. Brown,[a] Shuguo Ma,[b] and Linda S. Shimizu[a]*

[a]Department of Chemistry and Biochemistry, University of South Carolina, Columbia, South Carolina, 29208.

[b]College of Engineering and Computing, University of South Carolina, Columbia, South Carolina, USA.

shimizul@chem.sc.edu

Table of contents

Materials and Instruments: Triazinanone was prepared as previously described.[1] All chemicals were purchased from Aldrich and used without further purification. ^{1}H NMR and ^{13}C NMR spectra were recorded on Varian Mercury 400. The IR data were collected on Shimadzu 8400 FT-IR spectrometer in KBr cells of 0.2 mm to 1 mm path length. The electron spray mass spectra were obtained with Micromass Q-TOF I mass spectrometer. The X-ray powder diffraction data were collected on a Rigaku Dmax-2100 powder X-ray diffractometers using Bragg-Brentano geometry with CuKα radiation. The step scans covered the angular range 2-40° 2θ in steps of 0.05^{o}. Thermogravimetric analysis (TGA) for the guest desorption studies were carried out on 5-10 mg of I_2 absorbed sample using a TA instruments SDT-Q600. The TGA analysis was done at a heating rate of 4° C/min from 20 to 200° C under helium and then kept at 200° C (isotherm) for 10 minutes. UV-vis absorption studies were carried out using a Shimadzu UV-vis Spectrophotometer with 50mm and 10 mm precision cells made of Quartz Suprasil 300. The

scanning electron microscopy (SEM) image was recorded on FEI Quanta 200 ESEM with an accelerating voltage of 30 kV.

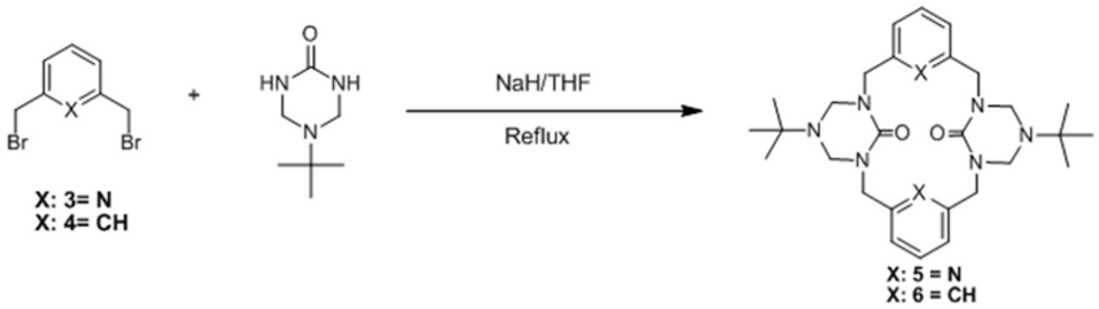

Scheme S1. Synthesis of triazinanone protected bis-urea macrocycles.

Triazinanone protected *bis*-urea macrocycle (5) A suspension of 5-(1,1-dimethylethyl) tetrahydro-1, 3, 5-triazin-2(1H)-one (1.00 g, 6.4 mmol) and NaH (460 mg, 19.2 mmol) in THF (300 mL) was heated to reflux in freshly distilled dry THF (100 mL) for 90 min. Then the solution was cooled to room temperature. A solution of 2, 6-*bis* (bromomethyl) pyridine **3** (1.69 g, 6.4 mmol) in THF (150 ml) was added drop wise over a 60 min period. The reaction mixture was heated at 75 °C for 48 h under nitrogen. Upon completion the reaction was quenched with 50 mL water and then reduced *in vacuo* to 75 mL. The solution was diluted with 50 mL water and then extracted with chloroform (3 × 100 mL). The combined organic layers were washed with brine and dried over anhydrous $MgSO_4$. Purification of crude reaction mixture by silica gel chromatography with a methanol : chloroform (1:9) eluent gave the product **5** as white solid (0.446 g, 27 %). Mp 237-240º C. ^{1}H-NMR (400MHz, DMSO-d_6), δ = 7.54 (t, J = 7.6 Hz, 2 H), 7.02 (d, J = 7.6 Hz, 4 H), 5.05 (dd, J =16.4, 11.6 Hz, 8 H), 4.35 (d, J = 11.6 Hz, 4 H), 3.92 (d, J =16.4 Hz, 4 H), 1.18 (s, 18 H); ^{13}C-NMR (100.56 MHz, DMSO-d_6) δ = 158.7, 154.5, 136.2, 119.5, 64.4, 53.7, 49.8, 28.6. HRMS (EI) Calculated for formula $C_{28}H_{40}N_8O_2$: [M+], 520.3274. Found *m/z* 520.3284.

Triazinanone protected *bis*-urea macrocycle (6) Triazinanone protected macrocycle **6** was prepared from the *tert*-butyl triazinanone and *meta* – α, σ-dibromoxylylene (**4**) according to the

method described by Dave *et al.*[2] ^{1}H- NMR (400 MHz, $CDCl_3$) δ = 7.41 (s, 2H),7.22 (t, *J* =7.4 Hz, 2H),7.0 (d, *J* =6.9 Hz, 4H), 5.68 (m, 4H), 4.15-4.35 (m, 8H), 3.65 (m, 4H),1.11 (s, 9H); ^{13}C NMR (100.56 Hz, $CDC1_3$) δ = 155.2, 138.7, 128.0, 126.4, 124.9, 62.2, 54.1, 48.5, 28.5.

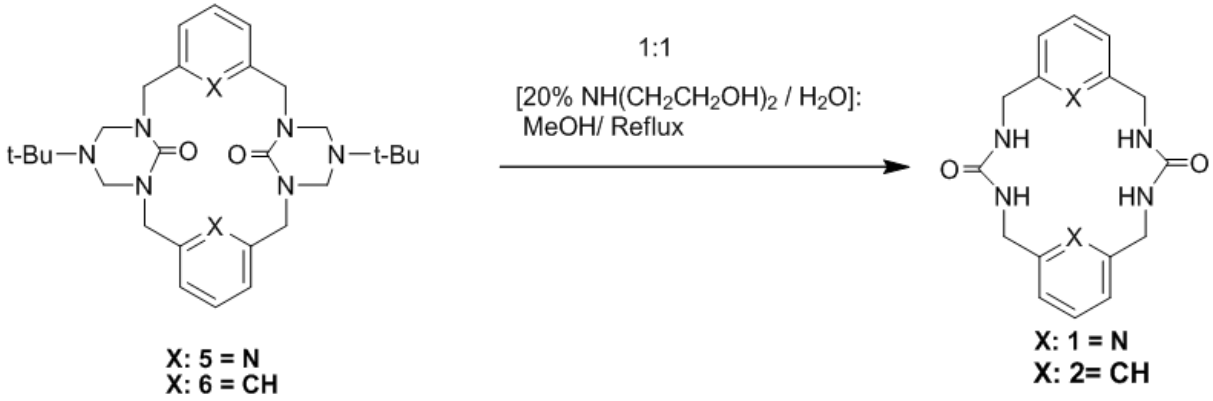

Scheme S2. Deprotection of triazinanone protected bis-urea macrocycles

Bis-urea macrocycle (1) Triazinanone protected *bis*-urea macrocycle (**5**) (0.290 g, 5.57 x 10^{-1} mmol) was heated to reflux in 40 mL of a 1:1 mixture of 20% [diethanolamine/water solution adjusted to pH ~ 2 with conc. HCl]: MeOH for 24 h. The methanol was removed *in vacuo* leaving an aqueous solution. A light brown solid precipitated upon cooling to room temperature. The solid was collected by suction filtration and washed with 45 mL H_2O. The filtrate was dried *in vacuo* to obtain the product as white powder (0.168 g, 93%). ^{1}H-NMR (400 MHz, DMSO-d_3) δ = 7.63 (t, *J* = 7.6 Hz, 2 H), 7.13(d, *J*= 8.1 Hz, 4 H), 6.91(br s, 4 H), 4.31(d, *J*= 5.4 Hz, 8 H); ^{13}C-NMR (100.56 MHz, $CDCl_3$) δ = 164.1, 155.1, 135.4, 123.7, 51.9. IR (cm^{-1}): 3426, 3328, 3269, 3054, 3030, 2908, 2730, 1990, 1660, 1568, 1456, 1386, 1106; HRMS (EI) calculated for formula $C_{16}H_{18}N_6O_2$: [M+], 326.3531. Found *m/z* 326.3529.

Bis-urea macrocycle (2) The *bis*-urea macrocycle (**2**) was prepared from triazinanone protected *bis*-urea macrocycle (**6**) according to the method described by Shimizu *et al.*[3] ^{1}H-NMR (400 MHz, DMSO-d_3) δ = 7.34 (t, *J* = 7.6 Hz, 2 H), 7.20(d, *J*= 8.1 Hz, 4 H), 6.49(s, 4 H), 4.61(br m, 4 H), 3.88 (br m, 4 H); ^{13}C-NMR (75 MHz, $CDCl_3$) δ = 158, 142.9, 128, 125.7, 123.9, 43.2. IR (cm^{-1}): 3365, 3306, 3033, 2915, 1627, 1587, 1450, 1421, 1303, 1262, 1200, 1056.

Recrystallization: Macrocycle **1** (50 mg) was stirred in DMSO (10 mL) in a pressure tube. The mixture was heated at 130°C for 2 h. Colorless block crystals of macrocycle **1** were obtained by vapor diffusion of methanol into DMSO.

Guest loading methods: The crystals of **1** and **2** were evacuated by heating at 120° C for 2 hours and cooled in desiccators to form the 'empty assembly'. All the loadings were carried out under sealed condition. Crystals of host **1** (50 mg) were added to a 20 mL scintillation vial and exposed to iodine vapor (12g) in a sealed vessel for between 1-9 days. Small amount (5 mg) of the solid material was taken to check the amount of iodine loaded in every 24 hours by TGA until the system reached equilibrium. The absorption of iodine was kinetically slow. Each time the vessel was sealed by high vacuum. The iodine species on the crystal surface were removed by sublimation at room temperature for 3 hours. Loading of the iodine vapor was time dependent and appeared to reach a maximum at 7 days.

Host **2** (35 mg) crystals were added to a 20 mL scintillation vial and exposed to iodine vapor (12g) in a sealed vessel for 1-12 days. Small samples (5 mg) of the solid material were checked by TGA every 24 h for 12 days. No weight loss was observed in any of the samples indicating that iodine was not absorbed.

TGA desorption studies: TGA analysis was carried out using TA instruments SDT Q600 on ~6 mg of crystalline material. The material was heated at 4 °C/min from 20 to 200 °C under helium gas and then kept at 200 °C for 10 minutes. Upon completion, the material was collected for the next absorption-desorption study. Host guest binding ratios were calculated using the formulas below. The average weight loss from six different absorption–desorption cycles of the host **1**•I_2 complex from different batches/ sizes of ground and ungrounded crystal was 18.9 ± 0.41 %. This corresponded to a host **1**:I_2 host: guest ratio 3:1 (Fig. S2).

$$\text{moles of host} = \frac{\text{Final weight g}}{326.3531\ \text{g/mol}}$$

$$\text{moles of guest} = \frac{\text{(Initial weight-final weight)}}{\text{Guest molecular weight}}$$

$$\text{Host : Guest} = \frac{\text{Host (mol)}}{\text{Guest (mol)}}$$

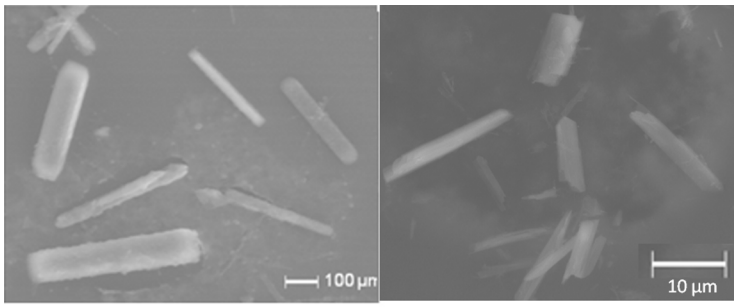

Fig. S1. Comparison of ground and unground crystals by FEI Quanta 200 ESEM: a) SEM image of intact host **1** crystal; b) SEM image of ground host **1**•I_2 whose size was estimated as ~2.8 µM x 9 µM.

Controls: To check the effect of surface area on guest binding, host **1** crystals were ground to a microcrystalline powder. The average size of the powder was estimated using SEM (Fig. S1). The powder was treated with iodine vapor in a sealed chamber for 7 days to form filled host **1**•I_2. Both the ground host **1** and unground host **1** showed similar uptake of iodine (Figure S2 and Figure 4a).

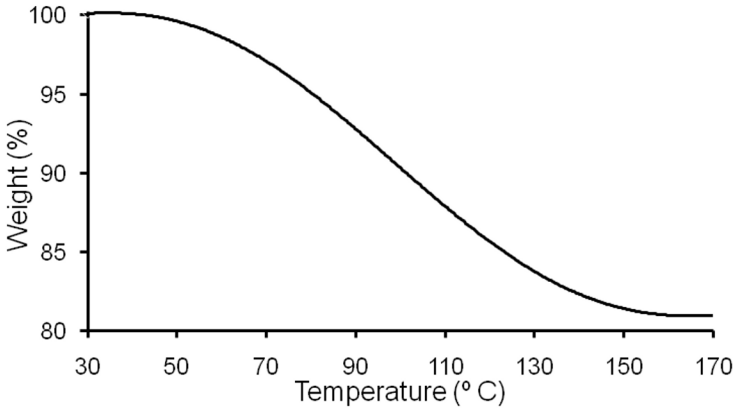

Fig. S2. A representative TGA desorption curve for ground Host **1**•I_2: A 19.05 % weight loss was measured by TGA, which corresponded to a loss of the I_2 guest. The calculated host **1**:I_2 stoichiometry was 3:1.

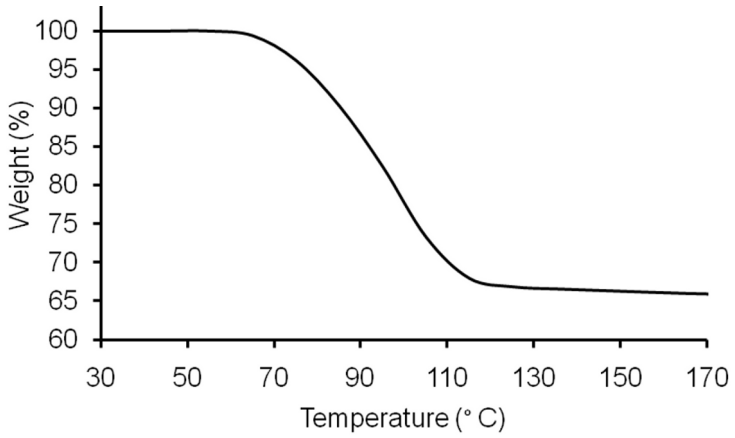

Fig. S3. TGA desorption curve for Host **1**•TFE: A 36.1% weight loss was measured by TGA between 60 and 120 °C, which corresponded to a loss of the TFE solvent. The calculated host **1**: TFE stoichiometry was 1:2.

Absorption Isotherm in Solution: Concentration variation equilibrium isotherms were carried out at 20 ± 2° C. Twenty different solution of iodine was prepared using ethanol as solvent. Concentration of iodine was varied from 0.05-50 mgL^{-1}. Absorbance of each solution was measured at 440 nm. Absorbance of each solution was plotted against the concentration of iodine in that solution to construct a Lambert-Beer plot (Figure S4). Using the Lambert-Beer plot, we determined the concentration of I_2 ethanol solutions.

Analysis of iodine binding: Host **1** (2 mg) was dispersed in each vial containing 10 mL I_2/ ethanol solution of concentration range 0.05-50 mg L^{-1}. After four days the iodine/ethanol solutions were centrifuged to remove the host sample and subsequently analyzed by UV-vis studies for their post absorption concentration at 440 nm (Figure S5). From the decrease in absorbance value for a particular concentration of iodine/ethanol solution after four days we calculated the amount of iodine adsorbed by 2 mg of sample. A larger 5 cm length UV was used for solutions that displayed UV-vis absorbance at 440 nm of < 0.02.

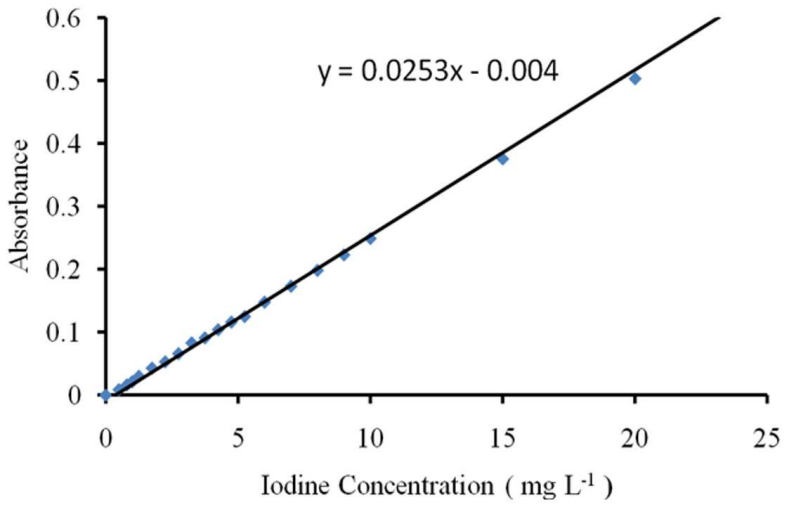

Fig. S4. Lambert Beer plot of iodine-ethanol solution versus iodine concentration

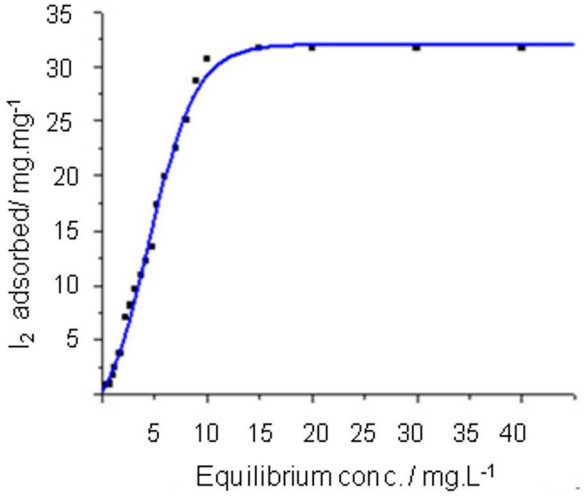

Fig. S5. Uptake of I_2 from an ethanol solution by host **1**.

XPS: XPS measurements were carried out on the Kratos AXIS Ultra DLD XPS system equipped with a hemispherical energy analyzer and a monochromated Al Kα source. The monochromatic Al Kα source was operated at 15 keV and 150 W. The pass energy was fixed at 40 eV for the detailed scans. The binding energy is calibrated using an Ag foil with $Ag3d_{5/2}$ set at 368.21 ± 0.025 eV for the monochromatic Al X-ray source.

Survey scans for **1** and **1**•I_2 complex are shown in fig. S6a and S6b respectively. The spectrum for **1** consists of three peaks the C 1s peak at 281.36 eV, the N 1s peak at 394.99 eV and O 1s peak at 326.73 eV. It was evident from the survey scan for **1**•I_2 complex that I_2 had

been incorporated into host **1** as indicated by the intense peaks centered at 615.18 and 626.46 eV due to iodine 3d electrons. Survey scans for physical mixture of host **1** and I_2 consisted of only C 1s, N 1s and O 1s peak. No peaks due to iodine 3d electrons were detected suggesting free I_2 was removed under high pressure of XPS. This result confirmed that iodine was strongly bound in **1**•I_2 complex.

Surface charge compensation causes the XPS peaks to shift to lower binding energies, therefore the measured peak position cannot be used to define the true oxidation states of elements. In order to define the oxidation state of iodine in the compound, we used the Auger parameter with NaI chosen as the reference sample (Fig. S6). The I MNN Auger line and I3d XPS spectrum for NaI were measured and obtained Auger parameter was compared with that for our sample. The NaI sample exhibited peaks at kinetic energies of 967.6 eV (6d) and the binding energy corresponds to this peak is 616.62 eV (6c). The difference between these two energy levels was 350.98 eV. In comparison host **1**•I_2 complex exhibited peaks at kinetic energies of 966.15 eV and the binding energy corresponds to this peak was 615.18 eV. The difference between these two energies is also 350.97 eV. Comparison of these two binding energies suggested that iodine was partially negatively charged in host **1**•I_2 complex and also indicated that only one type of iodine was present. Comparison between the nature of binding energy curves of X-ray induced iodine Auger emission of host **1**•I_2 complex and NaI also suggested that although the iodine was partially negatively charged its nature is different from I^-. This result also suggested the formation of charge transfer complex where iodine received a partial negative charge. In addition, the incorporated iodine molecules were not completely reduced to polyiodide chains (I_3^- or I_5^-) because no characteristic binding energy peaks that corresponds to polyiodide was detected in XPS survey. Also in UV-vis no characteristic peaks corresponds to I_3^- or I_5^- were generated. In addition, XPS showed only one type of iodine was present in the complex. Formation of polyiodide chains should show two types of iodine in XPS.

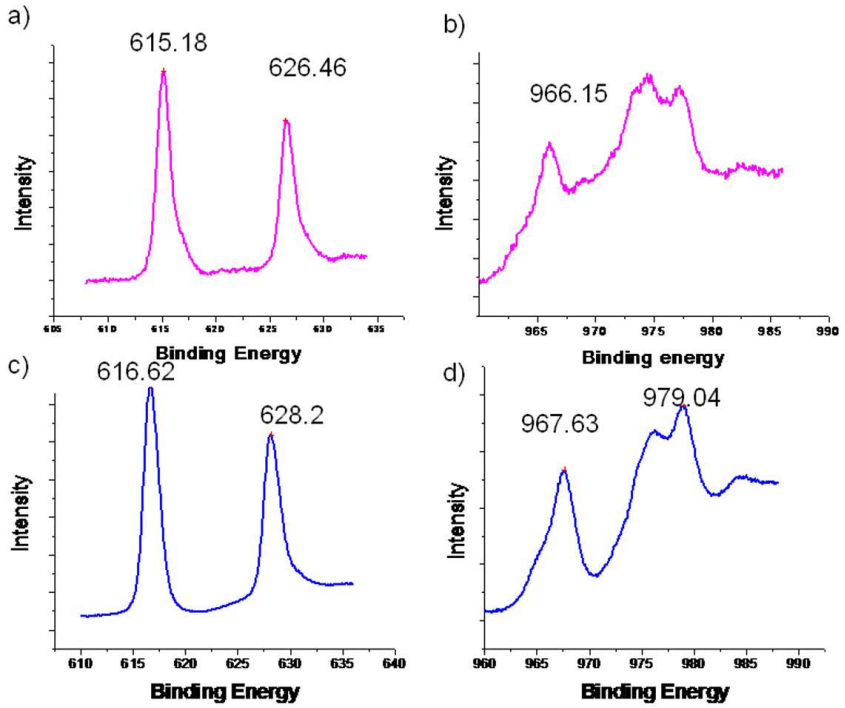

Fig. S6. a) I 3d XPS spectrum of **1**•I_2 complex; b) X-ray induced Auger emission spectrum over the I MNN region for **1**•I_2 complex; c) I 3d XPS spectrum of NaI; b) X-ray induced Auger emission spectrum over the I MNN region for NaI.

Fig S7 shows that 1s electron binding energy of the nitrogen is 394.99 eV, the binding energy shifts to 395.35 eV after the formation of the complex. The increase of the N 1s binding energy in the complex suggests a higher oxidation state of N atoms in the complex. This implies that a charge transfer has occurred from pyridine to iodine in the complex.

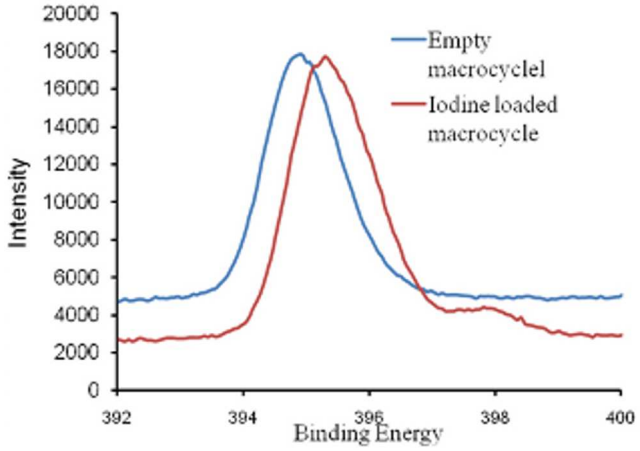

Fig. S7. XPS N1s spectra of empty host **1** and iodine loaded host (host **1**•I_2).

Powder X-ray diffraction (PXRD): Both freshly recrystallized empty crystals of **1** as well as iodine loaded crystals were ground to a powder and examined by PXRD. X-ray powder diffraction data was collected on a Rigaku DMAX-2100 powder X-ray diffractometers using CuKα radiation. The step scans data were collected at +0.05° steps in the angular range 2-40° 2θ at ambient temperature.

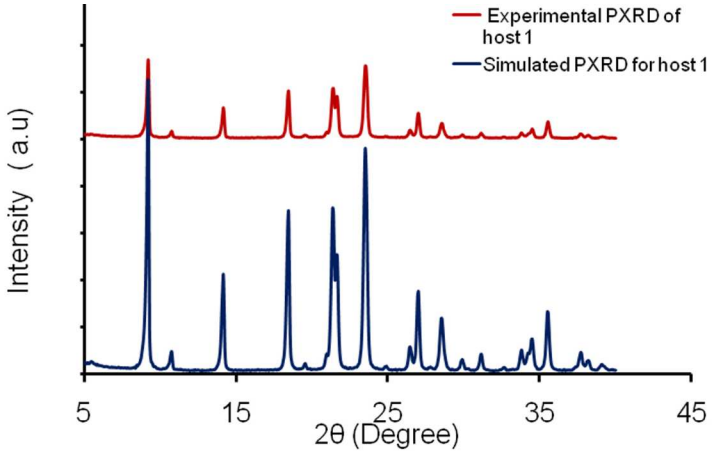

Fig. S8. Comparison of PXRD patterns of host **1**: Experimentally observed pattern (top); PXRD pattern simulated from the single crystal structure (cif file) using Powder cell (bottom).

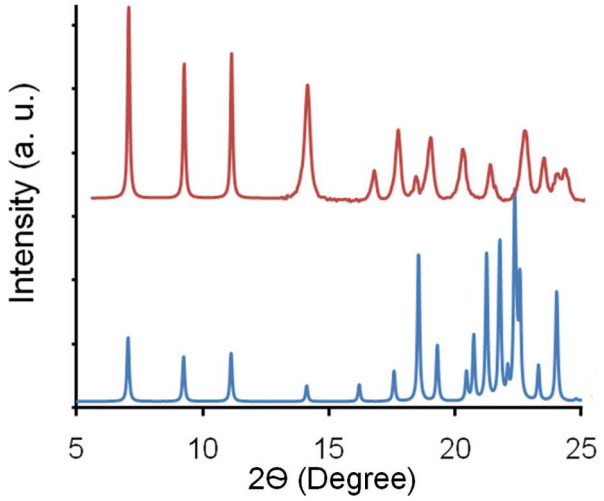

Fig. S9. Comparison of PXRD patterns of host **1•TFE**: Experimentally observed pattern (top); PXRD pattern simulated from the single crystal structure (.cif file) using Powder Cell.

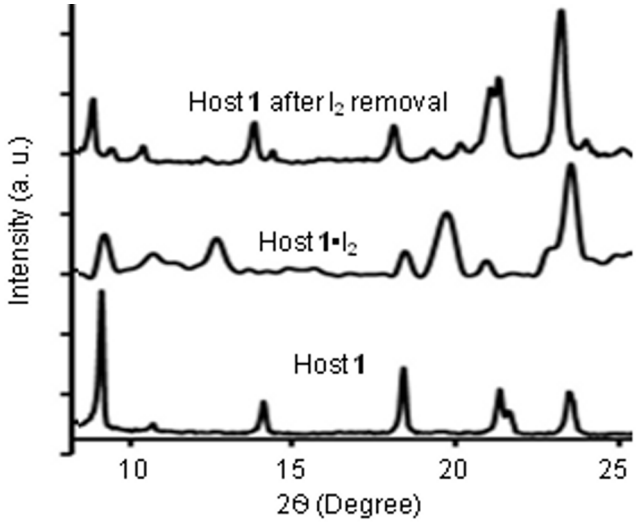

Fig. S10. Comparison of PXRD patterns of host **1** (bottom), Host **1**•I_2 (middle) and Host **1**•I_2 after I_2 removal (top).

Gas adsorption measurements

A clean and dry sample cell (6mm, large bulb) was measured on the balance first. Then approximately 35-50 mg of sample was transferred into the cell and the weight was recorded again. The sample containing cell was transferred to an Autoadsorb degassing unit. Samples were degassed for 12 h at room temperature. After gassing completed the cell was disconnected, reweighed on the balance, and the exact weight was recorded. Then the sample cell was transferred to the analysis station of Quantachrome instrument. The actual relative pressures range from 0.0003 to 0.03 for CO_2 and from 0.001 to 0.998 for H_2 after correcting the P_o value at 273 K. The volume pressure data thus obtained was reduced using Autosorb software for surface area, total pore volume, and pore size distribution calculations.

Table S1. Gas adsorption analysis for Host **1** with CO_2 (g)

P/Po	Volume [cc/g] STP	1/(W((Po/P)-1))
1.6307 E-03	0.2086	3.988 E+00
3.1829 E-03	0.4314	3.769 E+00
4.7433 E-03	0.6522	3.722 E+00
6.3025 E-03	0.8543	3.781 E+00
7.8620 E-03	1.0714	3.767 E+00
9.4241 E-03	1.3120	3.693 E+00
1.2530 E-02	1.6865	3.832 E+00
1.5649 E-02	2.0479	3.954 E+00
1.8755 E-02	2.4787	3.927 E+00
2.1828 E-02	2.8686	3.972 E+00
2.4997 E-02	3.2552	4.011 E+00
2.8125 E-02	3.6046	4.089 E+00

Slope = 1.04E+01

Y intercept = 3.74E+00

Correlation coefficient = 0.717252

C = 3.801 E+00

Table S2. Gas adsorption analysis for Host **1** with H_2 (g)

P/P_o	Volume [cc/g] (STP)
1.52E-02	2.734
2.02 E-02	3.093
2.52 E-02	3.447
3.02 E-02	3.793
4.02 E-02	4.409
5.02 E-02	4.913
6.02 E-02	5.593
7.02 E-02	6.022
8.02 E-02	6.507
9.02 E-02	6.865
9.98 E-02	7.431

Table S3. Gas adsorption analysis for Host **2** with CO_2 (g)

P/P_O	Volume [cc/g] STP	$1/(W((P_O/P) - 1)$
4.4183 E-03	0.8559	2.641 E+00
5.8747 E-03	1.1237	2.667 E+00
7.3264 E-03	1.4095	2.678 E+00
8.7838 E-03	1.6784	2.689 E+00
1.1671 E-02	2.1555	2.790 E+00
1.4581 E-02	2.6298	2.865 E+00
1.7488 E-02	3.1019	2.922 E+00
2.0401 E-02	3.5638	2.976 E+00
2.3316 E-02	3.9977	3.040 E+00
2.6206 E-02	4.5086	3.041E+00
2.8991 E-02	4.9221	3.089 E+00

Area = 1.454E+02 m^2/g

Slope = 1.726E+01

Y - Intercept = 2.495E+00

Correlation Coefficient = 0.979712

C = 7.918E+00

UV-vis analysis of host **1**•I_2 complex**:** To analyze the nature of host **1**•I_2 complex we scanned the UV-vis spectra of empty host **1** and host **1**•I_2 complex (Fig. S11). The empty host **1** showed absorbance at 278 nm which was blue shifted at 262 nm in host **1**•I_2 complex. Two new peaks appeared at 286 and 355 nm which were absent in empty host **1**. These two peaks are characteristic of iodine macrocycle charge transfer complex.

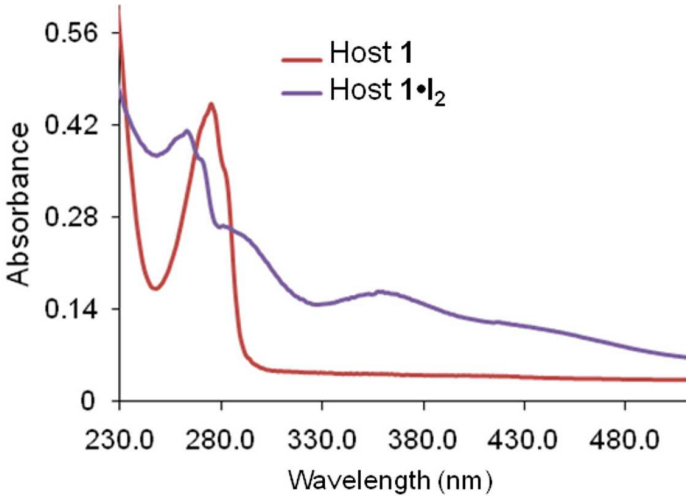

Fig. S11. UV-vis absorption spectra of host **1** and host **1**•I_2

Volume experiment: Host **1** (55 mg) was loaded in a one end open tube of 3 mm diameter. That tube was kept in a sealed iodine container. Volume of host **1** in tube was gradually expanded due to the vapor loading of iodine. We monitored the daily increase in volume by measuring the change in length (Figure S12). After 7 days 14% increase in volume was observed.

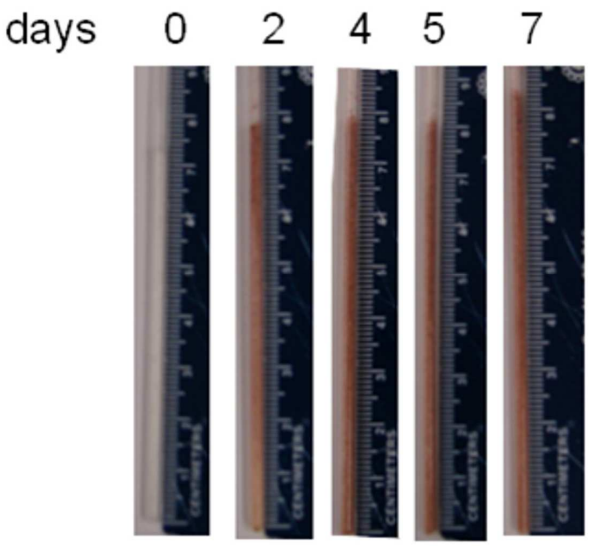

Figure S12. Change of volume of host **1** after adsorption of I_2. Change in volume was monitored after 2 days, 4 days, 5 days and 7 days.

X-Ray Structure Determination, $C_{16}H_{18}N_6O_2$ (1)

X-ray intensity data from a colorless block crystal were measured at 150(2) K on a Bruker SMART APEX diffractometer (Mo Kα radiation, λ = 0.71073 Å).[4] Raw area detector data frame integration was performed with SAINT+.[4] Final unit cell parameters were determined by least-squares refinement of 2525 reflections from the data set. Direct methods structure solution, difference Fourier calculations and full-matrix least-squares refinement against F^2 were performed with SHELXTL.[5]

The compound crystallizes in the space group $P2_1/c$ as determined by the pattern of systematic absences in the intensity data. The asymmetric unit consists of half of one molecule located on a crystallographic inversion center. All non-hydrogen atoms were refined with anisotropic displacement parameters. Hydrogen atoms bonded to carbon were located in difference maps before being placed in geometrically idealized positions and included as riding atoms with refined isotropic displacement parameters. Hydrogen atoms bonded to nitrogen were located and refined freely.

Table S4. Crystal data and structure refinement for host **1**.

Identification code	dimerdm	
Empirical formula	C16 H18 N6 O2	
Formula weight	326.36	
Temperature	150(2) K	
Wavelength	0.71073 Å	
Crystal system	Monoclinic	
Space group	$P2_1/c$	
Unit cell dimensions	a = 9.5207(5) Å	α= 90°.
	b = 4.6948(3) Å	β= 90.201(1)°.
	c = 16.3045(9) Å	γ = 90°.
Volume	728.77(7) $Å^3$	
Z	2	
Density (calculated)	1.487 Mg/m^3	
Absorption coefficient	0.104 mm^{-1}	
F(000)	344	
Crystal size	0.24 x 0.22 x 0.10 mm^3	
Theta range for data collection	2.14 to 26.37°.	
Index ranges	-11<=h<=11, -5<=k<=5, -20<=l<=20	
Reflections collected	8648	
Independent reflections	1489 [R(int) = 0.0502]	
Completeness to theta = 26.37°	100.0 %	
Absorption correction	None	
Refinement method	Full-matrix least-squares on F^2	

Data / restraints / parameters	1489 / 0 / 124
Goodness-of-fit on F^2	1.014
Final R indices [I>2sigma(I)]	R1 = 0.0352, wR2 = 0.0832
R indices (all data)	R1 = 0.0452, wR2 = 0.0875
Largest diff. peak and hole	0.223 and -0.162 e.Å^{-3}

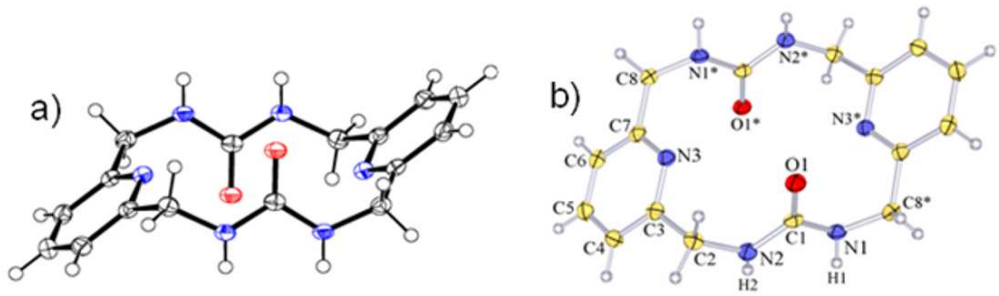

Figure S13. X-ray crystal structure host **1**a) Pyridyl rings parallel by symmetry b) Molecular structure. Centrosymmetric molecule. Displacement ellipsoids drawn at the 50% probability level. Symmetry code: * = 1-x, 1-y, 1-z.

X-Ray Structure Determination, $C_{16}H_{18}N_6O_2 \cdot 2(CF_3CH_2OH)$

X-ray intensity data from a colorless needle crystal were measured at 150(2) K on a Bruker SMART APEX diffractometer (Mo Kα radiation, λ = 0.71073 Å).[4] Raw area detector data frame integration was performed with SAINT+.[4] Final unit cell parameters were determined by least-squares refinement of 1146 reflections from the data set. The data were corrected for absorption effects with SADABS.[1] Direct methods structure solution, difference Fourier calculations and full-matrix least-squares refinement against F^2 were performed with SHELXTL.[5]

The compound crystallizes in the triclinic system. The space group $P\bar{1}$ was confirmed by the successful solution and refinement of the structure. The asymmetric unit consists of half of one $C_{16}H_{18}N_6O_2$ molecule located on a crystallographic inversion center and one badly disordered tri(fluoro)ethanol molecule of crystallization. The tri(fluoro)ethanol molecule was modeled with four independent positions with fixed occupancies of O1SA / O1SB / O2SA / O2SB = 0.35 / 0.20 / 0.25 / 0.20. These occupancies were set manually at values giving reasonable isotropic displacement parameters. Carbon and oxygen atoms in close proximity were assigned common displacement parameters, and all respective C-O, C-C, C-F, and F-F distances were restrained to be similar to one another (73 restraints). All non-hydrogen atoms were refined with anisotropic displacement parameters except for the disordered atoms (isotropic). Hydrogen atoms bonded to carbon were placed in geometrically idealized positions and included as riding atoms. The urea hydrogen atoms were located in difference maps and refined freely. A single position for the tri(fluoro)ethanol proton H1S was located, and its coordinates refined with U(iso,H) = 1.5U(iso, O1SA). The largest residual electron density peaks are in the tri(fluoro)ethanol molecule region. The high R-factors are because of the solvent disorder.

Table S5. Crystal data and structure refinement for host **1**•TFE

Identification code	ddtfes	
Empirical formula	C20 H24 F6 N6 O4	
Formula weight	526.45	
Temperature	150(2) K	
Wavelength	0.71073 Å	
Crystal system	Triclinic	
Space group	P $\bar{1}$	
Unit cell dimensions	a = 4.6955(12) Å	α = 93.970(5)°.
	b = 9.632(3) Å	β = 100.219(5)°.
	c = 12.775(3) Å	γ = 95.594(5)°.
Volume	563.7(2) $Å^3$	
Z	1	
Density (calculated)	1.551 Mg/m^3	
Absorption coefficient	0.142 mm^{-1}	
F(000)	272	
Crystal size	0.60 x 0.06 x 0.04 mm^3	
Theta range for data collection	1.63 to 24.94°.	
Index ranges	-5<=h<=5, -11<=k<=11, -15<=l<=15	
Reflections collected	5796	
Independent reflections	1970 [R(int) = 0.0583]	
Completeness to theta = 24.94°	99.7 %	

Absorption correction	Semi-empirical from equivalents
Max. and min. transmission	1.0000 and 0.6732
Refinement method	Full-matrix least-squares on F^2
Data / restraints / parameters	1970 / 73 / 201
Goodness-of-fit on F^2	1.045
Final R indices [I>2sigma(I)]	R1 = 0.0684, wR2 = 0.1698
R indices (all data)	R1 = 0.1004, wR2 = 0.1908
Largest diff. peak and hole	0.620 and -0.374 e.Å^{-3}

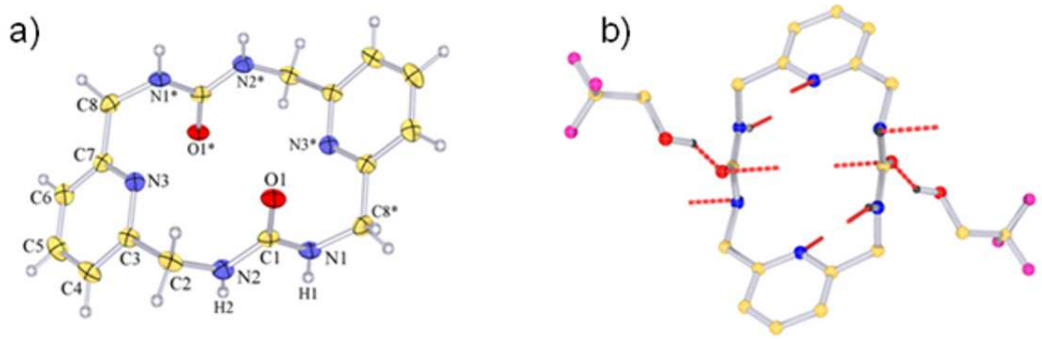

Figure S14. Views from the X-ray crystal structure of host **1**•TFE: a) Displacement ellipsoid plots of the cycle. Displacement ellipsoids are drawn at the 50% probability level. Symmetry code *= 1-x, 1-y, 1-z. Pyridyl rings parallel by symmetry. TFE omitted for clarity. b) Hydrogen bonding environment of the cycle, identical to solvent-free Host **1** structure except for TFE molecule H-bonded to carbonyl. Disorder in TFE is not shown.

1. A. R. Mitchell, P. F. Pagoria, C. L. Coon, E. S. Jessop, J. F. Poco, C. M. Tarver, F. D. Breithaupt, G. L. Moody, *Propellants, Explos. Pyrotech.* 1994, *19*, 232.

2. P. R Dave, G. Doyle, T. Axenrod, H. Yazdekhasti and H. L. Ammon, *J. Org. Chem.*, 1995, 60, 6946.

3. L. S. Shimizu, M. D. Smith, A. D. Hughes and K. D. Shimizu, *Chem. Commun.*, 2001, 1592.

4. SMART Version 5.630, SAINT+ Version 6.45 and SADABS Version 2.10. Bruker Analytical X-ray Systems, Inc., Madison, Wisconsin, USA, 2003.

5. Sheldrick, G. M. SHELXTL Version 6.14; Bruker Analytical X-ray Systems, Inc., Madison, Wisconsin, USA, 2000.

6. Sluis, P. v.d.; Spek, A. L. *Acta Crystallogr., Sect A* 1990, 46, 194-201.

7. (a) Spek, A. L. *Acta Crystallogr., Sect A* 1990, 46, C34. (b) PLATON, A Multipurpose Crystallographic Tool, Utrecht University, Utrecht, The Netherlands, Spek, A. L. 1998.